

---

## Stereo stitching deflectometry for measurement of specular surface with enlarged aperture

Ruiyang Wang<sup>1,2</sup>, Feng Gao<sup>1</sup>, Dahai Li<sup>2</sup>, Xiangqian Jiang<sup>1</sup>

<sup>1</sup>EPSRC Future Metrology Hub, University of Huddersfield, Huddersfield HD1 3DH, UK

<sup>2</sup>College of Electronics & Information Engineering, Sichuan University, Chengdu 610065, China

[r.wang2@hud.ac.uk](mailto:r.wang2@hud.ac.uk); [ryry.wang@qq.com](mailto:ryry.wang@qq.com);

---

### Abstract

The measurement aperture of deflectometry is limited by the line of sight from the camera to the screen: only the aperture through which the camera can see the pattern displayed on the screen can be measured. A marker-free stereo stitching deflectometry (SSD) is proposed to enlarge the measurement aperture. The sub-apertures are calculated with a stereo-iterative algorithm, and then stitched together to reconstruct a full-aperture result. The measured area is significantly enlarged compared to conventional stereo deflectometry. We test a high-quality optical flat with 190mm diameter using the proposed SSD and an interferometer. The measurement error of the SSD is below 100nm RMS in comparison to the measurement result of the interferometer.

Optical metrology, deflectometry, sub-aperture stitching

---

### 1. Introduction

Optical elements with specular surface, especially aspheric and free-form surfaces, have a variety of applications in modern optical systems, such as large astronomical telescope, imaging lens, head-up display system for driver assistance as well as the laser inertial confinement fusion facility etc. New design, manufacturing and testing techniques of aspheric and free-form surface provide larger field of view, larger numerical aperture, and better packaging performances. The deflectometry [1,2] is a very promising way to test specular surface, providing advantages such as non-contact, large dynamic range and high accuracy.

Deflectometry is a slope metrology based on the law of reflection, and the slope is further integrated to reconstruct the surface. The slope is measured by sensing the deflection of ray that is reflected off the surface of the unit under test (UUT). However, the problem called height-slope ambiguity needs to be addressed as the slope and height cannot be simultaneously determined without extra device or information. The solution for the ambiguity can be categorized into active deflectometry, passive deflectometry and mono-deflectometry. The active deflectometry [3-5] uses multiple screen locations to determine the source ray direction from screen, and the passive deflectometry [1,6,7] uses two-camera configuration to realize stereo measurement. The software configurable optical test system [8] or mono-deflectometry is developed to test specular surface with a single camera and fixed screen configuration, the height-slope ambiguity is solved by roughly knowing the nominal shape of the UUT.

The deflectometry can only measure specular surface with a limited size. To ensure the light emitted from the screen are reflected off the UUT and captured by the camera, either a very large screen is used or only a very small part of the UUT is measured. A common way to enlarge the testing aperture is sub-aperture stitching. The sub-aperture stitching in deflectometry is difficult as the cameras 'see' only the surroundings instead of

the UUT itself. Therefore, the markers on the UUT are used to identify the overlapping area between sub-apertures [9]. The markers can harm the surface quality of the UUT, this is undesirable in a non-contact optical testing.

A marker-free SSD for measurement of specular surface with enlarged measured aperture is proposed. The point cloud of the sub-aperture is measured based on a stereo-iterative reconstruction algorithm. And the sub-apertures from different camera views are stitched together with the stitching method. The theoretical basis is described in the second section. The experimental measurement is demonstrated in the third section. A high-quality optical flat with out-of-plane deviation below  $1/10$  wavelength is measured to demonstrate the measurement accuracy. The last section concludes the work.

### 2. Theory

The proposed SSD system consists of two cameras and a screen, the UUT is placed in front of the cameras and the screen, as shown in Fig. 1(a). The screen is used to display structure light patterns, such as sinusoidal fringe and randomly distributed speckle. The pattern is reflected off the specular surface of the UUT and captured by the cameras. With a limited size of the screen, each camera can observe the displayed pattern through a sub-aperture on the UUT, the captured images are illustrated in Fig. 1(a). The conventional passive deflectometry can only measure the overlapping area between sub-apertures while the proposed stitching deflectometry intends to measure the combined area of the sub-apertures, as shown in Fig. 1(b).

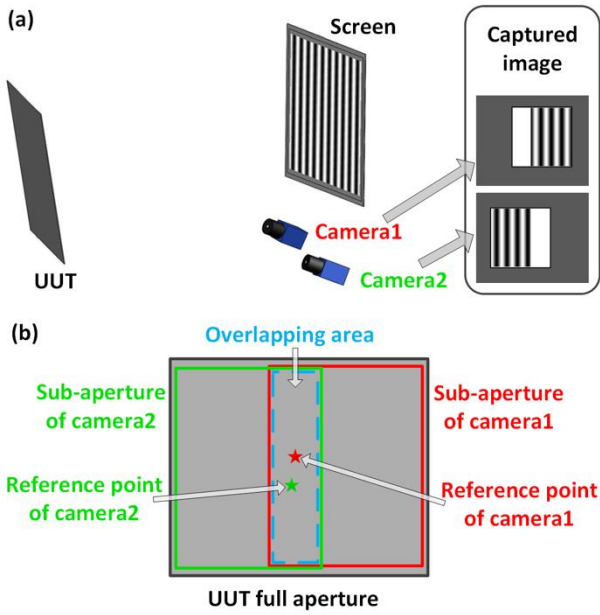


**Figure 1.** The schematic of (a) the stereo stitching deflectometry and (b) the sub-aperture stitching

The overall procedure of the SSD is as follows:

Step 1: Calibrate the deflectometric system. The internal matrixes of the cameras  $A_{cn}$ , distortion parameters of the cameras  $k_{cn}$ , the rotation and translation matrixes from screen coordinate to camera coordinate  $R_{s2cn}$  and  $T_{s2cn}$  are determined, the subscript  $n$  denotes the camera order. The calibration step is accomplished with Ren's method [10].

Step 2: Calculate sub-aperture point cloud. For each camera view, a reference point (RP) is selected, the three-dimensional position of which is determined by a stereo searching algorithm. As the point-by-point stereo searching is avoided, this algorithm is more computational efficient. Then based on the RP, the sub-aperture point cloud is calculated with an iterative reconstruction [11]. The combined method is referred to as the stereo-iterative algorithm. The details of the stereo-iterative algorithm can be found in reference [12,13].

Step3: Stitch the sub-apertures. The overlapping area is defined as the common area of the point cloud in sub-apertures, the stitching coefficient is calculated within the overlapping area by a fitting method. The stitching error between sub-apertures is then removed and the full-aperture height map is obtained. The stitching algorithm is detailed in reference [13]. The stitching model includes only the correction for piston and tilt for the sub-apertures.

### 3. Testing on an optical flat

An experimental setup is established to verify the marker-free SSD, as demonstrated in Fig. 2. The test system consists of an LCD screen with  $1200 \times 1600$  pixel, two cameras with  $966 \times 1296$  pixel and the UUT. A high-quality optical flat with out-of-plane deviation below  $1/10$  wavelength is measured to demonstrate the accuracy. The system parameters  $A_{cn}$ ,  $k_{cn}$ ,  $R_{s2cn}$  and  $T_{s2cn}$  are delicately calibrated before the measurement. The 8-step phase shifting algorithm and heterodyne temporal unwrapping algorithm are used to extract the phase distribution as well as the coordinates of screen source point. The Zernike polynomial is used as the polynomial set for modal integration method [14,15].

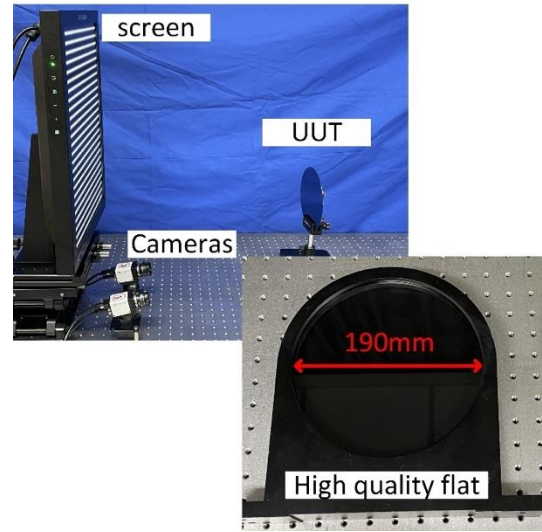


**Figure 2.** Experimental test system and UUT.

The captured fringe images from the two cameras are shown in Fig. 3. The selected reference points are obviously in the overlapping area. The sub-aperture calculation is conducted separately to obtain the point cloud datum, which are shown in Fig. 4. Then the stitching algorithm is used to provide the full-aperture, as illustrated in Fig. 5(a). Piston and tilt terms are removed from the height to show the out-of-plane deviation measured by the proposed method, as shown in Fig. 5(b), with 86.3nm RMS and 517.0nm PV. As comparison, the result measured by Fizeau interferometer is demonstrated in Fig. 5(c), with 6.0nm RMS and 40.1nm PV. The proposed stitching deflectometry can achieve 100nm error in RMS within an aperture of 190mm.

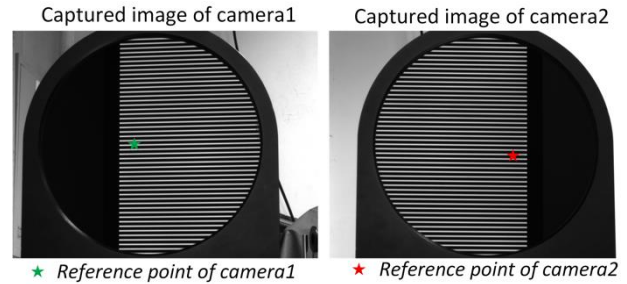


**Figure 3.** Captured images and the selected reference points.

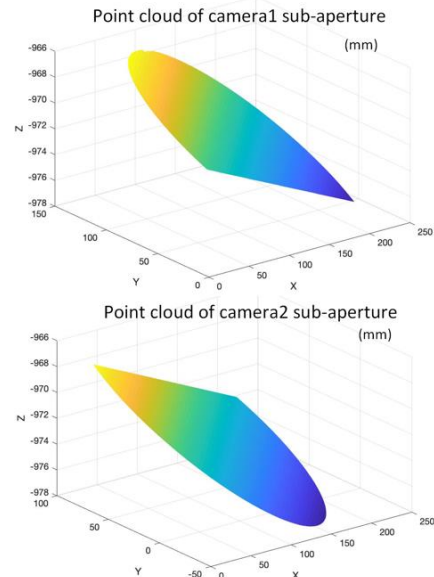


**Figure 4.** Sub-aperture point cloud of the two cameras.

Though delicate calibration is conducted, there is a nearly 100nm RMS difference. The comparison of zernike coefficient between stitching deflectometry and interferometer is given in Fig. 6. This error could arise from the sub-aperture calculation (systematic error) and/or the stitching algorithm. The systematic error is introduced by non-ideal setup, such as non-ideal camera model and imperfect screen with out-of-plane shape and refraction of the covering glass, etc. We remove the tilt and piston from Fig. 4 to demonstrate the shape of sub-aperture before the stitching, as shown in Fig. 7(a) and 7(b). Fig. 7(a) and 7(b) share identical features with Fig. 5(b), as well as the RMS and PV magnitude, indicating that the stitching hardly induces large errors. On the other hand, the stitching model includes

only piston and tilt, which in theory hardly introduces high-order error to the stitched aperture. We demonstrate the residual map in Fig. 7(c), the residual is at a similar order of magnitude to the systematic error. The residual map shows the difference excluding piston and tilt in the overlapping area, artifacts like the around 0.7 micrometer rise in the bottom-right corner are not fitted and stitched into Fig. 5(b). Therefore, the measurement accuracy is mainly affected by the systematic error introduced by non-ideal setup instead of the stitching algorithm. To further improve the measurement accuracy, either calibration of systematic error is required or imperfection of setup should be addressed.

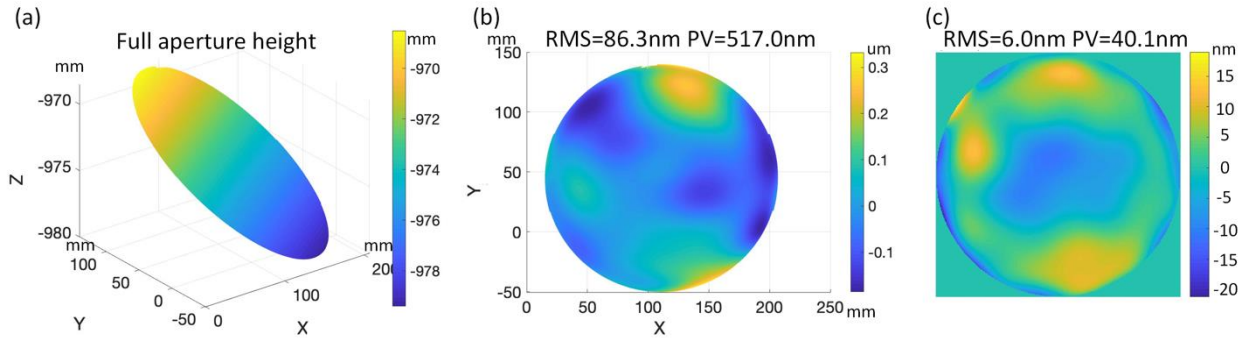


Figure 5. Results of stitching deflectometry: (a) full aperture height, (b) the result with piston and tilt removed, (c) interferometer result.

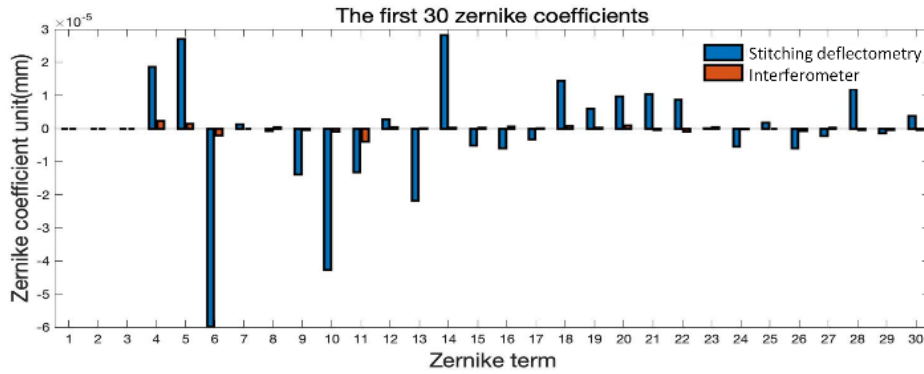


Figure 6. Comparison of the first 30 Zernike coefficient between the stitching deflectometry and interferometer, piston and tilt are removed.

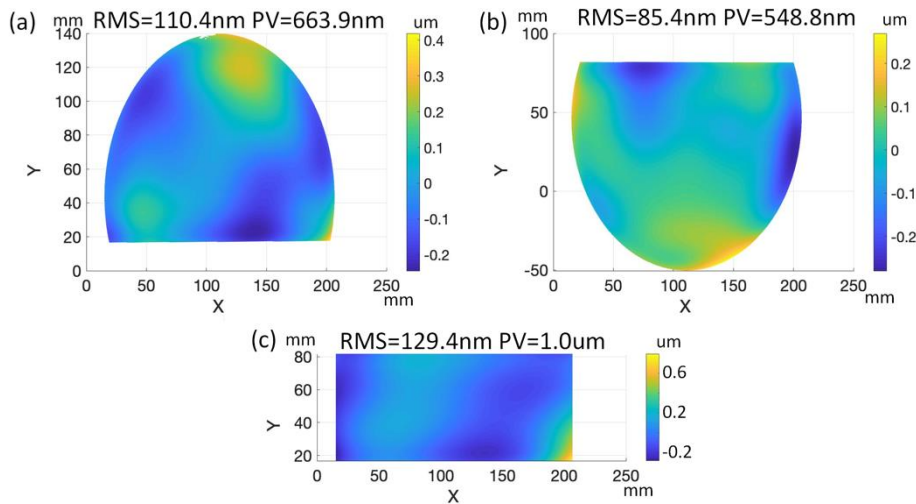


Figure 7. (a) Camera 1 sub-aperture shape with piston and tilt removed, (b) camera 2 sub-aperture shape with piston and tilt removed, (c) residual of stitching in the overlapping area.

#### 4. Conclusion

We propose a stereo stitching deflectometry that utilizes the ambiguity-free stereo-iterative algorithm and eliminates the use

of markers on the UUT. The stereo-iterative algorithm is a combination of stereo-algorithm for RP and iterative reconstruction, it is more efficient than the conventional stereo algorithm because the point-by-point stereo searching is

avoided. The calculated point cloud of sub-aperture identifies the overlapping area, which is used to further stitch the sub-apertures together. The stitched aperture is significantly larger than the measured area of the conventional deflectometry, especially passive deflectometry. We verify the proposed method with experimental measurements. A high-quality optical flat with 6nm RMS deviation (in 190mm aperture) is measured. The proposed stitching deflectometry measurement error is below 100nm RMS. With this method, the deflectometry can measure large size optics by extending the two-camera stitching to multi-camera stitching.

## Acknowledgements

The authors gratefully acknowledge the Chinese Government Scholarships (CSC), and the National Natural Science Foundation of China founding (U20A20215 and 61875142), and the Sichuan University funding (2020SCUNG205), and UK's Engineering and Physical Sciences Research Council (EPSRC) funding of "The EPSRC Future Advanced Metrology Hub" (EP/P006930/1), the funding of "A Multiscale Digital Twin-Driven Smart Manufacturing System for High Value-Added Products" (EP/T024844/1), and the funding of "Next Generation Metrology Driven by Nanophotonics" (EP/T02643X/1).

## References

- [1] Knauer M C, Kaminski J and Hausler G 2004 *Proc. SPIE* **5457** 366-376.
- [2] Bothe T, Li W, Kopylow C von and Juptner W P 2004 *Proc. SPIE* **5457** 411-422.
- [3] Petz M and Tutsch R 2005 *Proc. SPIE* **5869** 58691D.
- [4] Zhang X, Li D and Wang R 2021 *Optics express* **29**(18) 28427-28440.
- [5] Liu Y, Huang S, Zhang Z, Gao N, Gao F and Jiang X 2017 *Scientific reports* **7**(1) 1-8.
- [6] Xu J, Xi N, Zhang C, Shi Q and Gregory J 2010 *Optica Applicata* **40**(4) 827-841.
- [7] Zhang H, Šics I, Ladrera J, Llonch M, Nicolas J and Campos J 2020 *Optics express* **28**(21) 31658-31674.
- [8] Su P, Parks R E, Wang L, Angel R P and Burge J H 2010 *Applied optics* **49**(23) 4404-4412.
- [9] Chen P, Li D, Wang Q, Li L, Xu K, Zhao J and Wang R 2018 *Optics and Lasers in Engineering* **110** 392-400.
- [10] Ren H, Gao F and Jiang X 2015 *Optics express* **23**(17) 22060-22068.
- [11] Wang R, Li D and Zhang X 2021 *Measurement* **168** 108393.
- [12] Han H, Wu S, Song Z, Gu F and Zhao J 2021 *Optics Express* **29**(9) 12867-12879.
- [13] Wang R, Li D, Zhang X, Zheng W, Yu L and Ge R 2021 *Optics Express* **29**(25) 41851-41864.
- [14] Zhao C and Burge J H 2007 *Optics express* **15**(26) 18014-18024.
- [15] Zhao C and Burge J H 2008 *Optics express* **16**(9) 6586-6591.